It can be shown that Ψ's and Φ's, in this case, are given by

$$\Psi = r^4[(\tau k/4) + B_2 Q_2''(\nu)] \qquad \Psi' = Ar^4 \qquad (26)$$

$$\Phi = (4\mu c/i)[(\tau k\nu/4) + B_2 Q_2'(\nu)] \qquad \Phi' = 4Akc\mu\nu/i$$

where

$$\mu = \sin\eta \qquad \nu = i\sinh\xi$$

and A, B_2 are constants. They are given by Eq. (22) where ν_0 is now equal to $i\sinh\alpha$. The result obtained by Bhowmick[1] follows immediately from the preceding case when $G \to \infty$.

Case 3: $k = b/a$

Here we set

$$z' + ir = \rho e^{i\varphi} \qquad (27)$$

so that, on the surface equation (13),

$$\rho = a \qquad (28)$$

and Eq. (12) transforms into

$$\Psi_{,\rho\rho} + (1/\rho^2)\Psi_{,\varphi\varphi} - (2/\rho)\Psi_{,\zeta} - 3(\cot\varphi/\rho^2)\Psi_{,\varphi} = 0 \qquad (29)$$

Now for large ρ, condition (11a) being

$$\Psi \sim (\tau k/4)\rho^4(1 - \mu^2)^2$$

where $\mu = \cos\varphi$, we take a solution of Eq. (29) in the form

$$\Psi = (1 - \mu^2)^2[(\tau k/4)\rho^4 + B_2/\rho] \qquad (30)$$

Since Φ and Ψ can be shown to satisfy the following relations,

$$r^3\Phi_{,\rho} = (1/\rho)\Psi_{,\varphi} \qquad r^3\Phi_{,\varphi} = -\rho\Psi_{,\rho} \qquad (31)$$

we therefore have

$$\Phi = \mu\rho(\tau k - B_2/\rho^5) \qquad (32)$$

We take Ψ' and consequently Φ' in the forms

$$\Psi' = Ar^4 = A\rho^4(1 - \mu^2)^2 \qquad \Phi' = 4Ak\mu\rho \qquad (33)$$

Now $\rho = a$, $\Phi = \Phi'$, and $G\Psi' = kc_{66}\Psi$. These conditions lead to the following values of A and B_2:

$$A = (5\tau k^2/4) \cdot [c_{66}/(G + 4k^2 c_{66})]$$

$$B_2 = \tau k a^5 \cdot (G - k^2 c_{66})/(G + 4k^2 c_{66}) \qquad (34)$$

Stresses

The important stress component on the surface of the inclusion is

$$p_{n\theta} = (G/r^2) \cdot (\partial\Psi'/\partial s) \qquad (35)$$

where s is measured along a meridian arc on the surface of the inclusion, and n is the normal to this surface. Therefore,

$$p_{n\theta} = 2AGa^2 \sin2\zeta/(a^2 \cos^2\zeta + b^2 \sin^2\zeta)^{1/2}$$

where $\zeta = \eta$, or $\pi/2 - \eta$, or φ accordingly as k is less than, or greater than, or equal to b/a and the constant A is known in all the cases.

Reference

[1] Bhowmick, S. K., "Stress concentrations around a small rigid spheroidal inclusion on the axis of a transversely isotropic cylinder under torsion," AIAA J. 1, 1219–1220 (1963).

An Analysis of a Compressible, Turbulent Boundary Layer on a Chemically-Reacting Pyrolytic Boron Nitride Surface

M. D. Bowen*
The Lockheed-Georgia Company, Marietta, Ga.

AND

C. W. Gorton†
Georgia Institute of Technology, Atlanta, Ga.

Introduction

THE developments over the past few years in the production of pyrolytic materials by decomposition of gases have created a growing interest in this type of material. Intensive investigations have been conducted on pyrolytic graphite, and in many respects pyrolytic boron nitride is similar to pyrolytic graphite.[1] The differences in the hot pressed and pyrolytic forms of boron nitride (BN) are much larger than the corresponding differences in the sintered and pyrolytic form of graphite. Hot pressed BN is limited primarily by the low melting temperature of the binder, B_2O_3, and the rapid reaction of B_2O_3 with water vapor.[2] The pyrolytic form has removed this limitation and extended the useful temperature range considerably.

There are very few published reports on the oxidation phenomena of pyrolytic BN. Some experimental data are available from the manufacturers. This data is in the form of measured weight loss at various temperatures at 1-atm pressure and with low-velocity air flow. The effects of oxide films and nitrogen release in protecting the surface from oxidation cannot be evaluated from the data. Powers[3] has published the results of oxidation tests on both boron nitride and a titanium diboride-boron nitride composition, but the data was not suited for an accurate determination of mass-loss rate. A theoretical study of the combustion phenomena with laminar flow has been performed by Bowen and Gorton.[4]

In this work the reactions of a pyrolytic boron nitride surface and air with a turbulent, compressible boundary layer are analyzed. The latest available thermochemical data on the boron species are incorporated into the mass-transfer calculations. The pressure and temperature corresponding to saturation by B_2O_3 (at low temperatures) and B (at high temperatures) are determined. A comparison is given of the heat and mass transfer occurring for a range of U_L/U_E from fully turbulent to laminar flow.

Analysis

The equations for determining the element mass fractions K at the wall in terms of mass-transfer parameter B' and freestream concentrations may be obtained by modifying the method given by Lees[5] for a "pure element" surface.[4] It is further assumed in the present analysis that all chemical reactions occur at the wall, and the products of reaction are distributed through the gas boundary layer by diffusion. The composition at the wall is assumed frozen at the chemical equilibrium concentration for a given wall temperature. The gas mixture is assumed to be binary insofar as diffusion is concerned. Under these assumptions it can be shown that

$$\bar{K}_{ie}/\bar{K}_{iw} = B' + 1 \qquad (1)$$

* Scientist, Lockheed-Georgia Research Center.
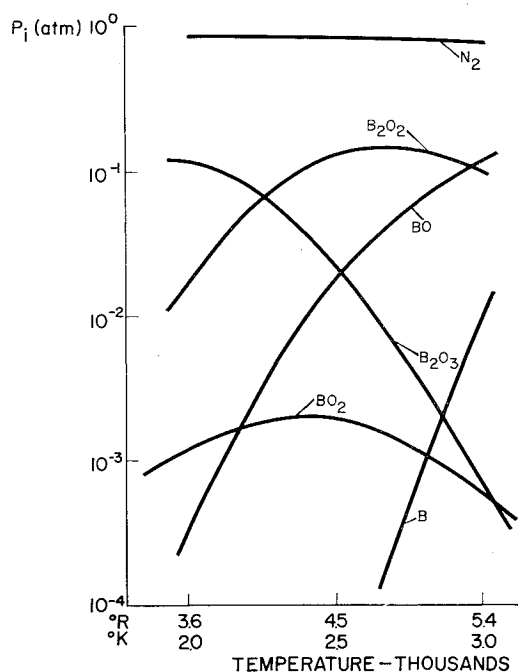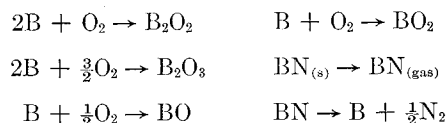† Professor of Mechanical Engineering.

Fig. 1 Species concentrations for $P_T = 1.0$ atm.

where i is any element not found in the surface material, and

$$\bar{K}_{i_w} = [B(M_i/M_{BN}) + \bar{K}_{i_e}]/[1 + B'] \quad (2)$$

The following reactions were considered as being the most significant:

$$2B + O_2 \rightarrow B_2O_2 \qquad B + O_2 \rightarrow BO_2$$

$$2B + \tfrac{3}{2}O_2 \rightarrow B_2O_3 \qquad BN_{(s)} \rightarrow BN_{(gas)}$$

$$B + \tfrac{1}{2}O_2 \rightarrow BO \qquad BN \rightarrow B + \tfrac{1}{2}N_2$$

By considering these reactions with the relationships given by Eqs. (1) and (2), one can obtain an independent equation relating the species partial pressures in the freestream to those at the wall:

$$[P_{N_2}/P_{O_2}]_e =$$
$$\left[\frac{2P_{N_2} - (P_B + P_{BO} + 2P_{B_2O_3} + P_{BO_2} + 2P_{B_2O_2})}{2P_{O_2} + P_{BO} + 3P_{B_2O_3} + 2P_{BO_2} + 2P_{B_2O_2}} \right]_w \quad (3)$$

Equation (3), Dalton's law, and the equilibrium constants for the reactions considered are sufficient to solve for the species concentrations at the wall for a particular pressure and temperature. The equilibrium constants were calculated from recently published data.[6]

The mass transfer may be calculated using the approach suggested by Dorrance.[7] From the preceding analysis the concentration of each of the species can be determined, and the mass-transfer parameter B' may be calculated from one of the intermediate equations used in obtaining Eq. (3). From Dorrance's work the following relationships were used in the BN calculations:

$$B' = \left[1 + \frac{B''C_{HC}}{C_f/2} \right] \left[1 + \frac{B''C_{HC}}{C_f/2} \frac{U_L}{U_E} \right]^{S-1} - 1 \quad (4)$$

$$B'' = \left[1 + \frac{B''C_{HC}}{C_f/2} \right] \left[1 + \frac{B''C_{HC}}{C_f/2} \frac{U_L}{U_E} \right]^{P-1} - 1 \quad (5)$$

The ratio U_L/U_E as used here is a weighting factor, which is descriptive of that portion of the boundary layer over which the laminar-flow transport properties predominate. The Schmidt and Prandtl numbers appearing in the equations are the laminar values. The desired relationship is found

by solving the preceding equations for each B' considered and for each value of U_L/U_E and S. The heat transfer may be determined by writing a heat balance at the solid-gas interface.[7] If thermal radiation is neglected and the specific heats of the gases assumed equal, the conducted heat flux in the solid may be written

$$\dot{q}_s = \rho_e u_e C_{Hc} \Delta I \left[1 + \left(\frac{C_{Hd}}{C_{Hc}} - 1 \right) \frac{h_c}{\Delta I} - \frac{B''L_v}{\Delta I} \right] \quad (6)$$

where

L_v = heat of vaporization
h_c = chemical potential
$\Delta I = (I_f)_r - (I_f)_w + h_c$

Results

Species concentration calculations were performed for a pressure range of 0.01 to 100 atm.[4] Figure 1 gives typical results for a pressure of 1 atm. The pressure effect on the condensible species, B_2O_3 and B, was determined by comparing the concentration data for the pressure range 0.01 to 100 atm. The concentration of B_2O_3 was found to fall rapidly with decreasing pressure, and at 0.01 atm the concentration remained below the saturation level over the entire diffusion-controlled region. Boron was found to increase rapidly for all pressures, but the curves were displaced to the higher temperatures at the higher pressures. This is a result of the pressure effect on the decomposition rate of BN. This also results in the concentration level of boron in the boundary layer reaching saturation at the higher temperatures.

The mass transfer (Figs. 2 and 3) is presented in terms of a dimensionless mass-transfer parameter for a freestream pressure of 1 atm and two values of Schmidt number. The points corresponding to saturation by B_2O_3 and B are located by the solid vertical lines. The points were determined by plotting the vapor pressure of B_2O_3 and B vs temperature with the partial pressure curves for the boron and B_2O_3 species concentrations. The intersection of the vapor-pressure curve with the species partial pressures was taken as the point where condensation was possible. With available data it was not possible to determine accurately the value of Schmidt or Prandtl numbers for the gas mixtures. For this reason two values of the Schmidt number were used in the calculations to show its effect. The rate-controlled re-
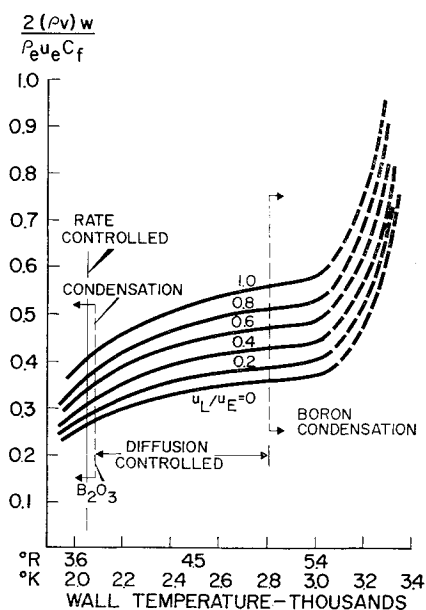

Fig. 2 Mass transfer for $P_T = 1.0$ atm, $S = 0.5$.

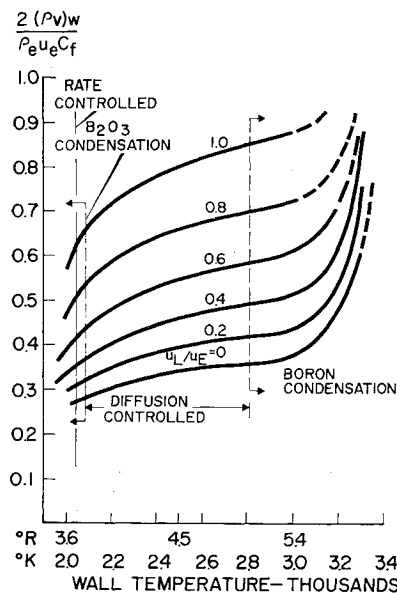$$\frac{2\,(\rho v)_w}{\rho_e u_e C_f}$$

Fig. 3 Mass transfer for $P_T = 1.0$ atm, $S = 0.7$.

gime is shown by a vertical, solid line. This was determined from mass-loss data supplied by a manufacturer of BN at 1.0 atm and with low-velocity air flow. It simply represents the temperature at which the weight-loss curve increases rapidly with temperature. The location of this point relative to the B_2O_3 saturation curve in Fig. 2 indicates a major part may be played by the oxide in protecting the surface at the lower temperatures, since the rate regime was determined from experimental data at 1.0 atm. Increasing the Schmidt number from 0.5 to 0.7, greatly reduced the effect of the weighting factor U_L/U_E on the mass-transfer parameter.

The heat transfer is presented in terms of a parameter, $-2\dot{q}_s/\rho_e u_e C_f$, as a function of wall temperature. Under the sign convention adopted, the negative value of the parameter is the heat that must be supplied to the wall to maintain the wall temperature. The heat-transfer calculations do not consider the possible condensation of B_2O_3 or boron. For the heat-transfer data presented here, the freestream temperature was taken as 537°R, and the kinetic-energy term in the enthalpy difference was neglected. The results are given in Fig. 4 for two pressures, 0.01 and 1.0 atm, two values of the weighting factor U_L/U_E, and for $P = 0.8$ and $S = 0.5$. The

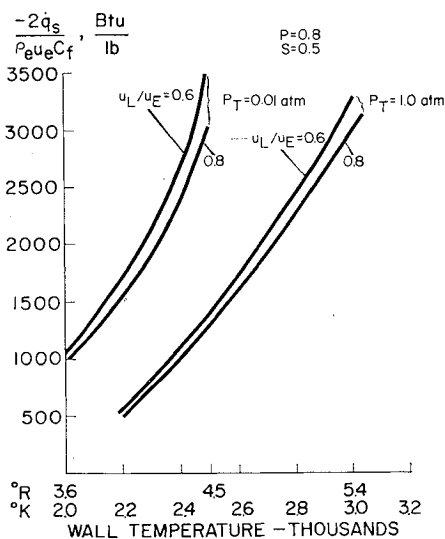$$\frac{-2\dot{q}_s}{\rho_e u_e C_f}, \frac{Btu}{lb}$$

Fig. 4 Heat-transfer parameter for $P_T = 0.01$ and 1.0 atm, $P = 0.8$, and $S = 0.5$.

relatively high slopes of these curves result from a decreasing contribution to the heat-transfer parameter from combustion and an increase in the decomposition rate with increasing wall temperature.

References

[1] Kotlensky, W. V. and Martens, H. E., "Tensile behavior of pyrolytic boron nitride to 2200°C," Nature 196, 1090–1091 (1962).

[2] Litz, L. M. and Mercuri, R. A., "Oxidation of boron carbide by air, water and air-water mixtures at elevated temperatures," J. Electrochem. Soc. 110, 921–925 (1963).

[3] Powers, D. J., "Static oxidation tests on boron nitride and on a titanium diboride-boron nitride composition," Bell Lab. Rept. 62-14(M), Revision A., Bell Aerosystems Co. (Oct. 1962).

[4] Bowen, M. D. and Gorton, C. W., "The combustion of pyrolytic boron nitride," AIAA Progress in Astronautics and Aeronautics; Heterogeneous Combustion, edited by H. G. Wolfhard, I. Glassman, and L. Green, Jr. (Academic Press, New York, 1961), Vol. 15, pp. 251–278.

[5] Lees, L., Combustion and Propulsion, Third AGARD Colloquium (Pergamon Press, New York, 1959), pp. 451–498.

[6] McBride, B. J., Heimel, S., Ehlers, J. G., and Gordon, S., "Thermodynamic properties to 6000°K for 210 substances involving the first 18 elements," NASA SP-3001 (1963).

[7] Dorrance, W. H., Viscous Hypersonic Flow (McGraw-Hill Book Company, Inc., 1962), pp. 206–242.

Specular and Lambert Reflection Problems in Radiation Dynamics

STEPHEN N. FALKEN* AND CHENG-TING HSU†
Iowa State University, Ames, Iowa

I. Introduction

IN space that is free of the gravitational and geomagnetic fields of celestial bodies, vehicles will still experience external forces such as those due to solar radiation. For space missions requiring precise trajectory control, the effects of these external forces must be accounted for. Cotter[1] and Dugan[2] have surveyed the dynamics of solar sails under the condition of specular reflection. Specular reflection is a simple, mirror-like reflection, which corresponds to no interaction between the radiation and the surface. Another simple reflection, which does not require a model used for interaction, is the Lambert reflection. The Lambert process, which diffusely reflects the incident radiation uniformly in all directions, contrasts with the specular process as two rather extreme limits in reflection processes. The present note aims to compare the dynamic effects on bodies due to these two limiting cases. The lift and drag coefficient of a flat plate, a circular cylinder, and a sphere in a parallel, incident radiation field will be evaluated for comparison.

II. Dynamic Forces in a Radiation Field

The energy and momentum contained in a volume V of an electromagnetic field in empty space may be written in gaus-